Citation: Molecular Therapy — Oncolytics (2015) **2,** 15008; doi:10.1038/mto.2015.8

www.nature.com/mto

ARTICLE

ATN-224 enhances antitumor efficacy of oncolytic herpes virus against both local and metastatic head and neck squamous cell carcinoma

Ji Young Yoo[1], Jun-Ge Yu[2], Azeem Kaka[2], Quintin Pan[2], Pawan Kumar[2], Bhavna Kumar[2], Jianying Zhang[3], Andrew Mazar[4], Theodoros N Teknos[2], Balveen Kaur[1] and Matthew O Old[2]

Head and neck squamous cell carcinoma (HNSCC) is the sixth most frequent cancer worldwide, and the 5-year survival rates are among the worst of the major cancers. Oncolytic herpes simplex viruses (oHSV) have the potential to make a significant impact in the targeted treatment of these patients. Here, we tested antitumor efficacy of RAMBO, an oHSV armed with the antiangiogenic Vstat120, alone and in conjunction with ATN-224, a copper chelator against HNSCC *in vitro* and *in vivo* animal models. We found that all tested HNSCC cells responded well to virus treatment and were sensitive to RAMBO-mediated oncolytic destruction. *In vivo*, RAMBO had a significant antiangiogenic and antitumorigenic effect. Physiologic levels of copper inhibited viral replication and HNSCC cell killing. Chelation of copper using ATN-224 treatment significantly improved serum stability of RAMBO and permitted systemic delivery in HNSCC tumor xenografts models. Furthermore, our results show that the combination of ATN-224 and RAMBO strongly inhibits lung metastases in a mouse model of HNSCC. These findings suggest that combining ATN-224 with RAMBO has potential for clinical trials in both early and advanced HNSCC patients.

Molecular Therapy — Oncolytics (2015) **2**, 15008; doi:10.1038/mto.2015.8; published online 20 May 2015

INTRODUCTION

Head and neck squamous cell carcinoma (HNSCC), which occurs in the oral cavity, oropharynx, larynx, and hypopharynx, is the sixth most common cancer worldwide and the 5-year survival rates are among the worst of the major cancer. There are over 35,000 new cases of oral and oropharyngeal squamous cell carcinomas diagnosed in the United States each year, resulting in 12,000 deaths.[1] Currently, patients with locally advanced stage I/II of HNSCC are treated with surgery, radiotherapy, chemotherapy, and molecular targeted therapies.[2] Despite initial clinical responses, 50% of these patients relapse and develop advanced and metastatic disease. Despite significant improvements in the therapy, the long-term survival rates in patients with advanced stages of HNSCC have not increased significantly. Treatment often leads to severe and permanent functional deficits with a negative impact on patients' quality of lives.[3] Therefore, there is a great need for the development of novel therapies to improve survival of recurrent and metastatic HNSCC patients while limiting treatment-related toxicities.

Oncolytic herpes simplex viruses (oHSV) are genetically engineered to specifically replicate in tumor tissue and avoid infection and propagation in normal cells.[4] oHSV have shown antitumor efficacy *in vitro* and *in vivo* animal models of head and neck cancers.[3,5,6] In the few clinical trials investigating safety of oHSV administered to patients, no dose-related toxicities were identified.[3] However, complete responses or therapeutic efficacy have rarely been observed; so, significant improvements in oHSV therapy are necessary. Currently, there are two HSV-1-derived oncolytic viruses that are being tested for safety and efficacy in patients with head and neck cancers (NCT01017185, and NCT00931931).

Angiogenesis has a well-recognized role in HNSCC progression, resistance to drugs, and radiotherapy. Many clinical trials have been conducted with antiangiogenic agents in this disease, even if they often showed limited efficacy.[7] Copper is an essential cofactor for the function of many angiogenesis-promoting enzymes and plays a key role in multiple steps along the angiogenesis pathway, leading to the activation of many molecules involved in angiogenesis.[8] Furthermore, raised serum copper concentrations were observed in nearly 40% of the HNSCC patients.[9] Therefore, copper suppression therapy may improve HNSCC patient survival. Apart from supporting angiogenesis, serum copper also inhibits wild-type HSV infection and replication via DNA damage induced by copper (II) ions. Additionally, strategies to combat tumoral angiogenesis have been

[1]Department of Neurological Surgery, Dardinger Laboratory for Neuro-Oncology and Neurosciences, The Ohio State University Comprehensive Cancer Center and Wexner Medical Center, Columbus, Ohio, USA; [2]Department of Otolaryngology-Head and Neck Surgery, The James Cancer Hospital and Solove Research Institute, Wexner Medical Center at The Ohio State University, Columbus, Ohio, USA; [3]Center for Biostatistics, Department of Biomedical Informatics, The Ohio State University, Columbus, Ohio, USA; [4]Chemistry of Life Processes Institute and Robert H. Lurie Comprehensive Cancer Center, Northwestern University, Evanston, Illinois, USA. Correspondence: M Old (matthew.old@osumc.edu) or B Kaur (Balveen.kaur@osumc.edu)
Received 5 February 2015; accepted 21 March 2015

shown to improve oHSV therapy.[10,11] Tetrathiomolybdate (TM) functions by creating a complex with copper and serum albumin, effectively restricting cellular uptake of copper and has shown to strongly suppress increases in inflammatory and immune-related cytokines. TM has been approved by FDA for the treatment of Wilson's disease and is currently under investigation in several Phase II trials as an antiangiogenic and antineoplastic agent in a variety of cancers (NCT00383851 and NCT00405574, respectively). ATN-224 is a second-generation analog of TM that is orally available and has superior stability and a faster onset of action. While angiogenesis plays a significant role in the progression of HNSCC, the impact of oHSV in combination with antiangiogenic strategies has not been tested in preclinical or clinical HNSCC. We have previously shown that copper inhibit oHSV and sequestration of copper by ATN-224 is effective in reducing angiogenesis and synergizing unarmed oHSV therapy for glioma.[12] Here, we show for the first time that RAMBO, an oHSV armed with the antiangiogenic Vstat120,[12] has therapeutic efficacy against several different SCC models *in vitro* and *in vivo* and is significantly enhanced with copper chelation. Using a spontaneously metastasizing model of SCC, we show that RAMBO is an effective therapeutic modality for SCC tumors and that ATN-224 treatment synergizes with RAMBO, by both increasing antitumor effects of injected tumor and also by reducing metastasis in the lungs. These results suggest the potential of combining ATN-224 with oHSV for future clinical trials for patients with HNSCC. We plan to pursue phase 1 clinical trials and these findings have the potential to provide a significant framework for doing so.

RESULTS

RAMBO is cytotoxic and antiangiogenic toward human squamous cell carcinoma (SCC) cells

Vstat120 is the cleaved and secreted extracellular fragment of brain-specific angiogenesis inhibitor 1 (BAI1), and has been shown to be a potent antiangiogenic and antitumorigenic factor. Oncolytic herpes simplex virus (oHSV) RAMBO is an antiangiogenic Vstat120 expressing oncolytic virus. First, we tested the expression of Vstat120 in SCC cells infected with RAMBO. Western blot analysis using CAL27 and UM-SCC-74A cells treated with phosphate-buffered saline (PBS), control virus rHSVQ1, or RAMBO showed efficient production of Vstat120 in cells infected with RAMBO (Figure 1a). Next, we compared antitumor efficacy of rHSVQ1 and RAMBO in subcutaneously implanted CAL27 xenograft model. When CAL27 tumor size reached a volume of around 150 mm^3, animals were injected intratumorally with 1×10^6 pfu of rHSVQ1 or RAMSO and then were closely monitored for tumor growth. There was significant increase in progression free survival in RAMBO-treated mice compared to rHSVQ1 (*P*

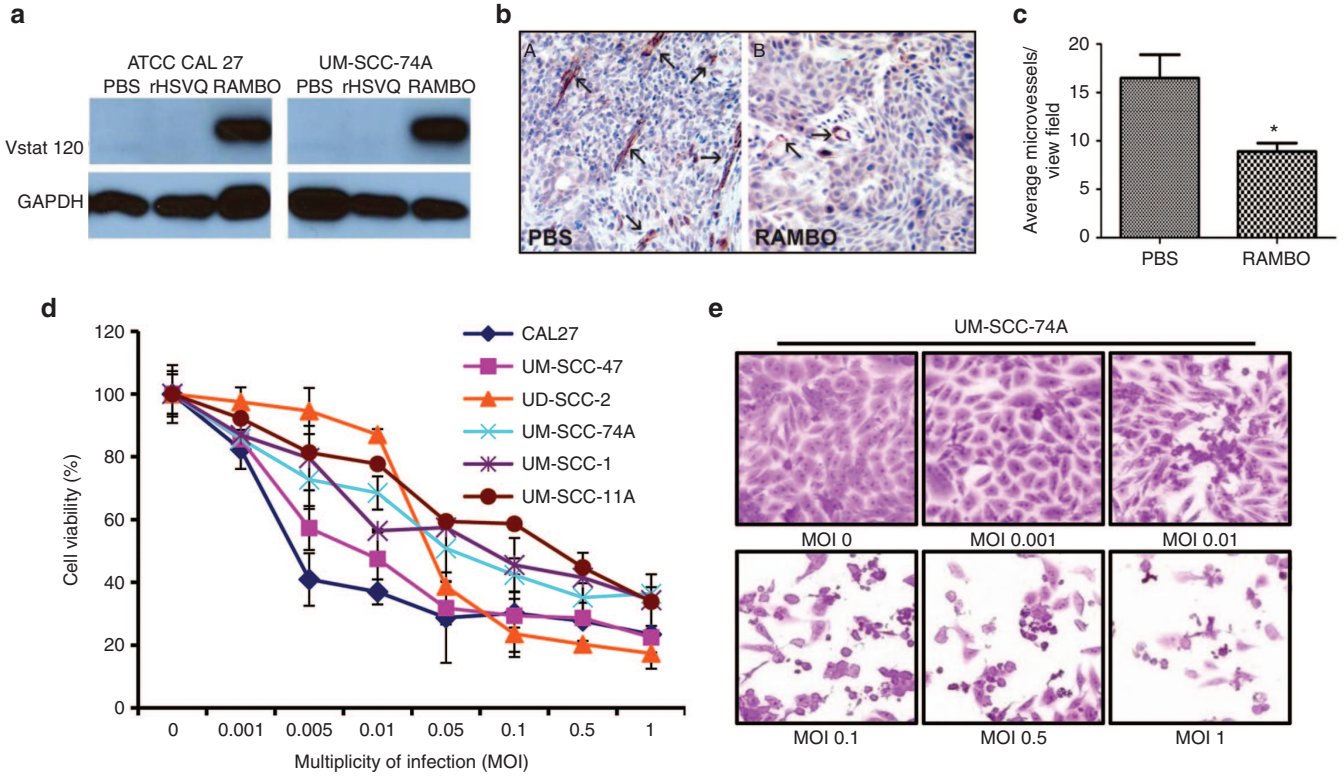

Figure 1 RAMBO is antiangiogenic and cytotoxic toward human squamous cell carcinoma (SCC) cells. (**a**) Western blot analysis of CAL27 and UM-SCC-74A cells treated with PBS, rHSVQ1, or RAMBO. The cells were harvested at 48 hours postinfection and analyzed for expression of Vstat120. GAPDH was used as a loading control. Note the presence of Vstat120 in cells infected with RAMBO. Data are representative results from a total of three separate experiments. (**b,c**) Antiangiogenic effect of RAMBO in CAL27 xenografts tumors. (**b**) Representative images of tumor sections illustrating microvessel density assessment stained with CD31 antibody. Arrows are representative vessels from each group ($n = 3$/group). (**c**) Quantification of CD31 immunostained vessels performed. Data shown are average vessel density ± SD ($P < 0.05$). (**d,e**) SCC cells are sensitive to RAMBO *in vitro*. (**d**) Quantification of cell viability of six different SCC cell lines infected with RAMBO relative to uninfected cells at the indicated multiplicity of infection (MOI) 48 hours postinfection. Data shown are % cell viability relative to uninfected cells and representative results from a total of three separate experiments. Data were analyzed by the paired student's *t*-test and error bars indicate ± SD for each group. (**e**) Representative images of UM-SCC-74A cells 48 hours after RAMBO infection at the indicated MOI. Note the rounded morphology and reduced attachment of infected cells 48 hours postincubation.

= 0.0201) (Supplementary Figure S1). To evaluate whether RAMBO could efficiently inhibit angiogenesis in SCC tumors *in vivo*, CAL27 subcutaneous tumor bearing mice were treated with PBS or RAMBO (2×10^6 plaque forming units (pfu)) via intratumoral injection. Seven days post-treatment, harvested tumors were analyzed for changes in microvessel density. Figure 1b shows a significant reduction in micro vessel density in tumors treated with RAMBO compared to PBS, confirming the antiangiogenic effects of Vstat120 ($P < 0.01$) (Figure 1c). Next, we tested the susceptibility of SCC cell lines to RAMBO mediated cell killing. Six human SCC cell lines (UM-SCC-74A, UM-SCC-1, UM-SCC-11A, UM-SCC-47, UD-SCC-2, and CAL27) were infected with RAMBO at the indicated multiplicity of infection (MOI), and cell viability was measured 48 hours postinfection (Figure 1d,e). All the tested SCC cells were highly susceptible to cell killing by RAMBO.

RAMBO shows significant antitumor effects against SCC tumors *in vivo*

Therapeutic efficacy of RAMBO was next examined in CAL27 SCC xenograft model in nude mice. When the subcutaneously implanted CAL27 tumors reached an average size of 200 mm^3 in volume, mice were randomized and PBS or RAMBO (2×10^6 pfu) was intratumorally injected on day 7 and day 16 (n = 6/group). Figure 2a shows tumor growth of individual mice treated with PBS or RAMBO. All tumors in PBS treated mice grew rapidly and all animals had to be sacrificed by day 42 due to tumor burden. In marked contrast, all mice treated with RAMBO showed significant delay in tumor growth after treatment by day 20. Furthermore, one mouse showed a complete response while the rest of the mice showed progressive disease after a partial response or stable disease (as measured by increasing tumor volume). Twenty-one days after initiation of ATN-225 treatment, a significant reduction in average tumor volume in animals treated with RAMBO was observed (Figure 2b). PBS-treated mice had large bloody tumors with visible hemorrhaging, while RAMBO-treated mice had smaller tumors which did not appear bloody or hemorrhagic compared to control tumors (Figure 2c). Kaplan–Meier survival curves of mice treated with PBS or RAMBO showed a significant improvement in median survival of RAMBO-treated mice (median survival of 27 versus 46 days, for PBS- and RAMBO-treated animals respectively, P value = 0.0045) (Figure 2d).

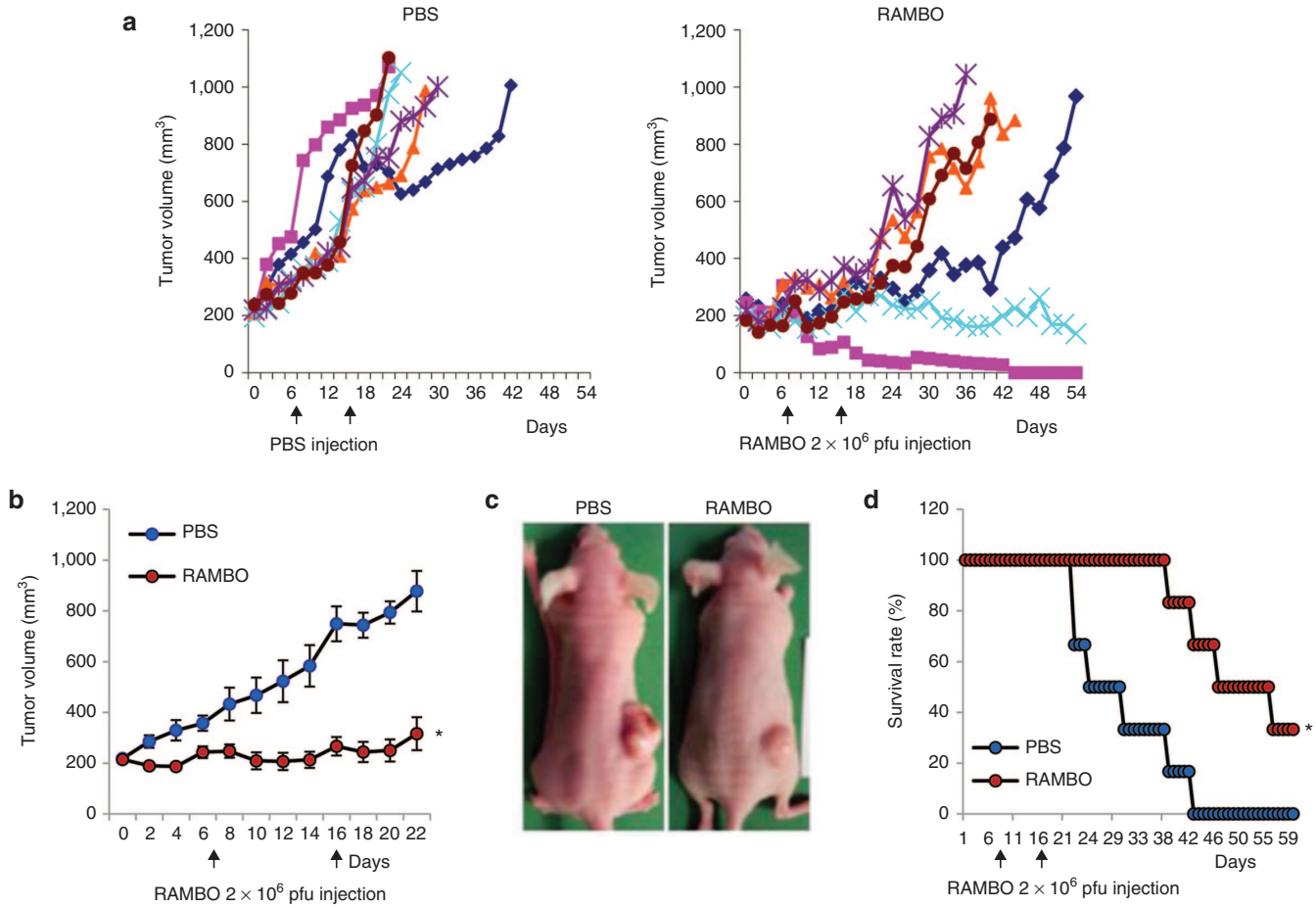

Figure 2 Antitumor efficacy of RAMBO against CAL27 SCC flank model. Athymic nude mice were subcutaneously implanted with CAL27 cells. When tumor size reached a volume of around 150 mm^3, animals were injected intratumorally with PBS or 1×10^5 pfu of RAMBO. Tumor volume was measured regularly after treatment. (**a**) Tumor growth in individual mice treated with PBS (left panel) or RAMBO (right panel) over a period of time after treatment. (**b**) Average tumor volume of mice treated with PBS or RAMBO over periods of study. Data points represent the mean of the tumor size for each group at the indicated time points. (**c**) Representative images of CAL27 tumor bearing mice treated with PBS or RAMBO. (**d**) Kaplan-Meier survival curves of the data in (**b**). The percentage of surviving mice was determined by monitoring the death of mice over a period of 60 days. *$P < 0.05$ compared with mice treated with PBS. The arrow indicates the time of treatment with RAMBO.

Physiologic level of copper inhibits RAMBO-mediated SCC cell killing and ATN-224 rescues its effect

We have previously shown that physiologic levels of copper can inhibit oHSV replication and killing of glioma cells.[12] To test whether copper could inhibit RAMBO mediated killing of SCC cells, we measured the viability of UM-SCC-74A cells infected with RAMBO with and without copper. Figure 3a demonstrates that the ability of RAMBO to destroy UM-SCC-74A cells is significantly reduced when treated with physiologic levels of copper. Quantification of viable cells revealed a dose dependent and significant reduction in cell viability of cells treated with RAMBO (Figure 3b). Average physiologic human levels of copper are above 10 µmol/l and complete inhibition of RAMBO-mediated cell killing was observed when RAMBO was treated with amounts greater than 10 µmol/l copper. Since copper inhibits oHSV activity *in vitro*, we tested whether copper chelation with ATN-224 could rescue RAMBO-mediated oncolytic SCC cell killing. Oncolytic efficacy of RAMBO treated with copper in the presence or absence of ATN-224 was tested by measuring the viability of UM-SCC-74A cells (Figure 3c). Crystal violet staining of viable cells shows efficient oncolysis of cells treated with RAMBO in the absence of copper (Figure 3c, top panel lane 2). However, the addition of copper eliminated the ability of RAMBO to kill UM-SCC-74A cells (Figure 3c, top panel lane 4). The addition of ATN-224 at concentrations of 8 µmol/l or higher showed complete rescue of RAMBO's oncolytic affects (Figure 3c, top panel lanes 10–12). In the absence of copper, ATN-224 did not affect oncolytic ability of RAMBO to destroy UM-SCC-74A cells *in vitro* (Figure 3c, bottom panel lane 5–12). Quantification of viable cells revealed that ATN-224 treatment efficiently rescued copper-mediated inhibition of RAMBO cell killing in multiple SCC cells (Figure 3d).

ATN-224 rescues copper-mediated inhibition of RAMBO replication *in vitro*

To evaluate whether the inhibition of RAMBO induced SCC cell killing by copper was due to inhibition of viral replication, we measured the viral replication in the presence and absence of copper and ATN-224 (Figure 4). As RAMBO encodes GFP, fluorescence microscopy was utilized to visualize GFP positive RAMBO-infected cell. Copper found in serum has been shown to inhibit wild-type HSV infection, and its topical use is currently being evaluated as an antiherpetic agent in patients with herpes skin lesions.[13–15] Consistent with these previous reports, a complete absence of GFP-positive cells was apparent when cells were infected in the presence of copper. However, the

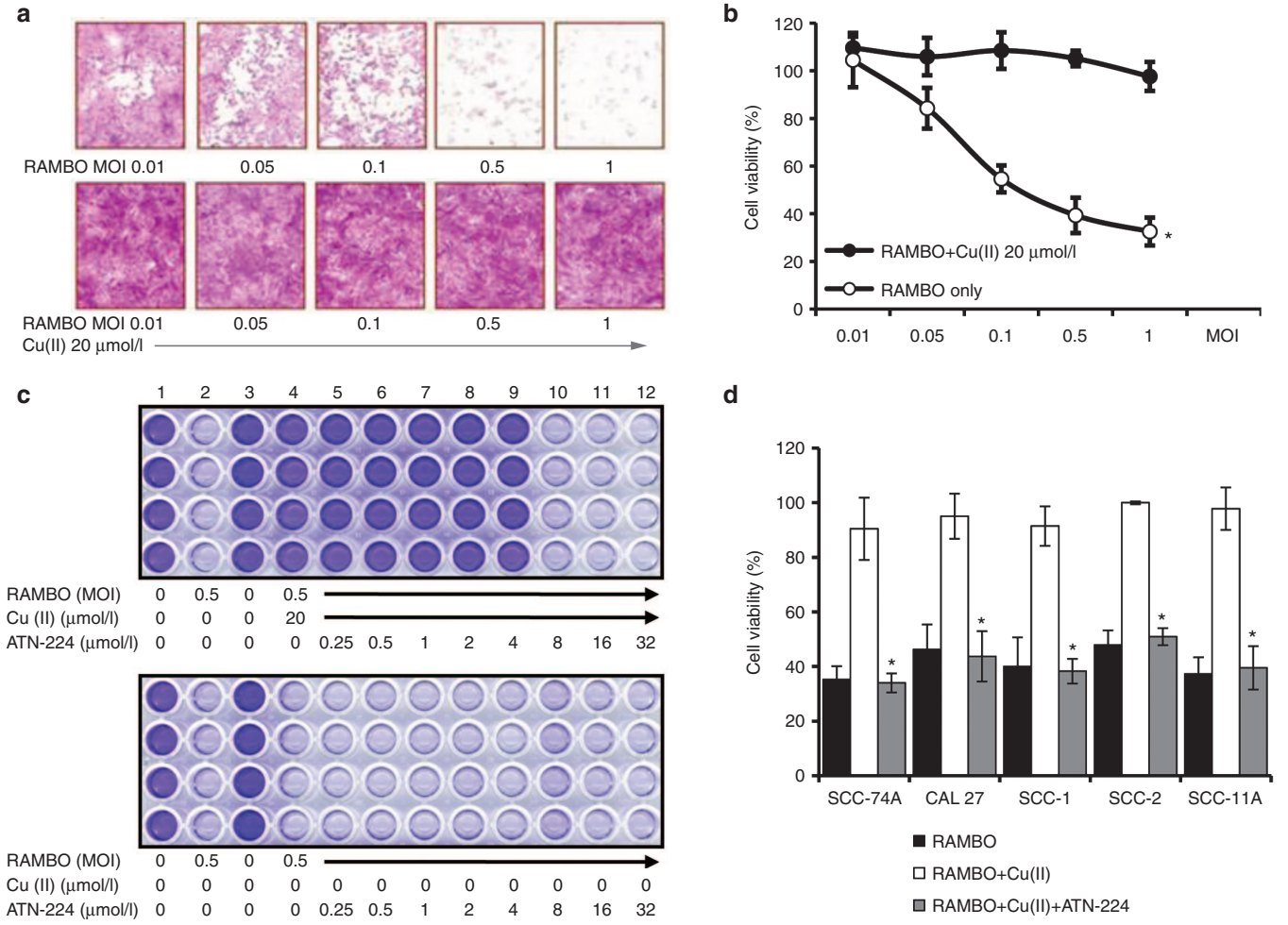

Figure 3 Copper-mediated inhibition of SCC cell killing induced by RAMBO is rescued by ATN-224. (**a**) Microscopic images of crystal violet stained UM-SCC-74A cells infected with RAMBO ± copper. (**b**) Quantification of cell viability of UM-SCC-74A cells infected with RAMBO at the indicated MOI ± physiologic levels of copper. (**c**) Images of crystal violet stained UM-SCC-74A cells infected with RAMBO treated with ATN-224 in the presence (upper panel) or absence (bottom panel) of copper. (**d**) Quantification of cell viability of the indicated cells infected with RAMBO at the indicated MOI ± copper in the presence or absence of ATN-224. Copper mediated reduced SCC cell killing induced by RAMBO was significantly rescued by ATN-224. Data shown are representative results from a total of three separate experiments. Data were analyzed by the paired student's t-test and error bars indicate ± SD for each group. *indicates *P* value <0.05.

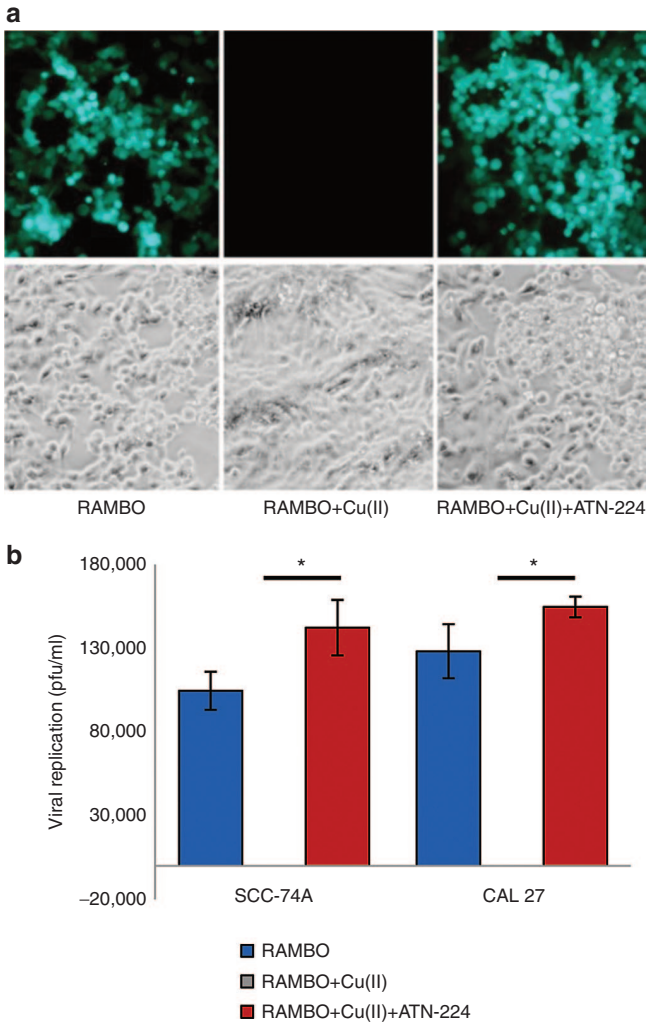

Figure 4 ATN-224 rescues copper-mediated inhibition of RAMBO replication *in vitro*. UM-SCC-74A cells were infected with RAMBO (0.1 MOI) alone or RAMBO (0.1 MOI) incubated with copper ± ATN-224. (**a**) Representative fluorescent microscopy images of GFP-positive infected cells indicating the presence of viral replication. (**b**) Quantification of viral titers produced by the indicated SCC cells infected with RAMBO ± copper in the presence or absence of ATN-224 *in vitro* (0.1 MOI, copper 20 µmol/l + ATN-224 32 µmol/l). Two days postinfection, the virus was harvested from infected cells and quantified by a standard plaque assay on Vero cells. Data shown are representative results from a total of three separate experiments. Data were analyzed by the paired student's *t*-test and error bars indicate ± SD for each group. *indicates *P* value <0.05.

ATN-224 treatment completely reversed the copper-mediated inhibition of RAMBO replication (Figure 4a). Consistent with GFP results, quantification of virus titers of RAMBO incubated with or without copper in the presence or absence of ATN-224 showed that copper completely inhibited the ability of RAMBO to replicate but ATN-224 rescued this effect ($P < 0.05$) (Figure 4b).

ATN-224 rescues copper-mediated inhibition of RAMBO replication *in vivo*

To test the *in vivo* relevance of these findings, we first tested whether ATN-224 treatment of mice could reduce serum copper levels. Ceruloplasmin (Cp) is a copper-containing oxidase, synthesized in the liver and circulating in blood, and serum Cp measurements have been used to follow copper depletion.[16] Mice were fed with ATN-224 or PBS by daily gavage for 6 weeks and blood was collected from submandibular vein weekly. Figure 5a shows a significant reduction in Cp levels in the serum from mice treated with ATN-224 compared to mice treated with PBS, indicating reduced serum copper levels ($P < 0.001$) (Figure 5a). Furthermore, suppression of copper levels was maintained up to 6 weeks. No obvious side effects were noted in long-term ATN-224 usage. Next, we tested whether reduction of serum copper in mice fed with ATN-224 could rescue the serum-mediated inhibition of the replication ability of RAMBO. Serum from mice treated with PBS or ATN-224 for 14 days was collected and incubated with RAMBO for 1 hour and the ability of RAMBO to replicate was measured by a standard plaque assay on vero cells. Viral titers were significantly enhanced when RAMBO was incubated with serum derived from ATN-224-fed mice compared to PBS-fed mice ($P < 0.001$) (Figure 5b). Next, we further evaluated whether ATN-224 treatment would improve the serum stability of RAMBO *in vivo*. Mice treated with ATN-224 or PBS for 10 days received RAMBO (2×10^7 pfu) via tail vein injection. Twenty minutes later, mouse serum was harvested and the amount of infectious viral particles was evaluated by a standard plaque assay on vero cells (Figure 5c). Figure 5c shows a significant increase in infectious virus particles that survived in samples treated with serum from ATN-224-treated mice compared with that from PBS-treated control mice ($P < 0.001$). Finally, we tested whether ATN-224 treatment of mice permitted for systemic RAMBO delivery. Tumor bearing mice were treated with single intravenous injection of RAMBO (5×10^6 pfu), and 2 days later mice were sacrificed and tumors were analyzed both by visualizing and by quantifying the number of viral gene copies in tumors. Significantly more RAMBO was found in tumors of mice treated with ATN-224 (Figure 5d,e), confirming significant enhancement of systemic oHSV delivery and viral replication. Collectively, these results suggested that ATN-224 could increase serum stability of RAMBO and enhance its systemic delivery efficacy.

Combination treatment with ATN-224 and RAMBO increases antitumor efficacy *in vivo*

Since increased tumor growth is associated with higher serum copper levels[17] and copper sequestration has been shown to have some therapeutic efficacy,[18] we evaluated the therapeutic efficacy of ATN-224 in two phenotypically different types of SCC (UM-SCC-74A and CAL27) xenograft models established in nude mice. UM-SCC-74A is a rapidly growing SCC cell line, while CAL27 has a slower growth rate. When the subcutaneously implanted CAL27 tumors reached an average size of 150 mm^3 in volume, mice were randomized and ATN-224 (0.7 mg/day) or PBS was systemically administrated via daily gavage ($n = 10$/group) until finishing experiment. At day 7 from ATN-224 or PBS daily gavage, animals were injected intratumorally with RAMBO (1×10^5 pfu) or PBS and tumor growth was measured twice a week (Figure 6a,b). As presented in Figure 6a, control tumors which received PBS showed rapid tumor growth, leading to a tumor volume of 663 ± 72.5 mm^3 by day 15. In contrast, the mean tumor volumes in mice treated with RAMBO, ATN-224, or ATN-224 plus RAMBO were 211.1 ± 23.5, 346.2 ± 34.9, and 138.9 ± 18.5, respectively. These data correlate to 68.2, 47.8, and 79.1% tumor growth inhibition, respectively, as compared to PBS control. By day 60 following treatment, 80% of the animals in the ATN-224 plus RAMBO-treated group were still viable as compared to 0, 30, and 30% in the PBS-, RAMBO-, and ATN-224-treated groups, respectively (Figure 6b). The tumor growth suppression that was observed in the CAL27 xenograft tumor model was also observed in the rapidly growing subcutaneous UM-SCC-74A xenograft model ($n = 7$/group) (Figure 6c,d).

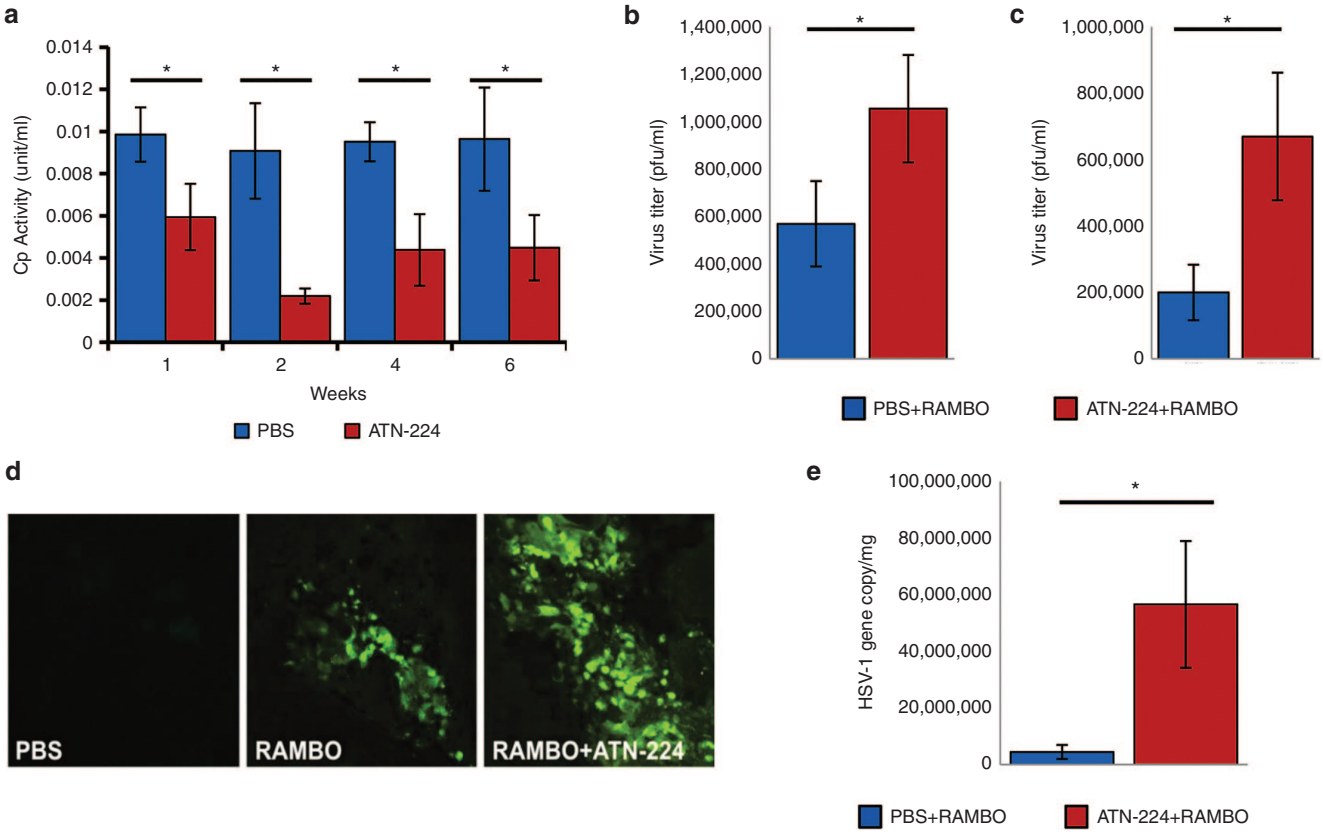

Figure 5 ATN-224 treatment of mice reduces serum-mediated inhibition of copper and rescues virus replication *in vivo*. (**a**) Serum ceruloplasmin levels in UM-SCC-74A tumor bearing mice at indicated time points after initiation of treatment with ATN-224 or PBS by daily gavage (PBS $n = 5$; ATN-224 $n = 6$). Data were analyzed by the paired student's *t*-test and error bars indicate ± SD for each group. (**b**) Serum mediated inhibition of virus replication is rescued by ATN-224 *ex vivo*. Serum from mice fed ATN-224 or PBS for 14 days was collected and incubated with RAMBO for 1 hour at 37 °C. Virus titer was then calculated by a standard plaque assay using Vero cells, ($P < 0.01$). Data were analyzed by the paired student's *t*-test and error bars indicate ± SD for each group ($n = 7$/group). (**c**) Serum-mediated inhibition of virus replication is rescued by ATN-224 *in vivo*. CAL27 tumor bearing mice treated with PBS or ATN-224 by daily gavage for 10 days were injected with RAMBO (5×10^6 pfu) via tail vein. Twenty minutes postinjection, the amount of virus present in serum was measured by a standard plaque assay on Vero cells. Data shown are the mean pfu/ml in serum of mice ± SD. Virus titer was significantly increased in ATN-224-treated serum than PBS-treated serum (PBS $n = 6$; ATN-224 $n = 5$) ($P < 0.01$). (**d,e**) ATN-224 treatment increased systemic delivery of RAMBO to tumors *in vivo*. CAL27 subcutaneous tumor bearing mice were fed with PBS or ATN-224 by daily gavage and injected with RAMBO (5×10^6 pfu) intravenously by tail vein injection on day 14. Two days later from RAMBO injection, tumors were harvested and analyzed for viral gene copy. (**d**) Fluorescent microscopy images of GFP-positive infected tumor tissues. More GFP-positive cells were present in tumors treated with RAMBO and ATN-224 when compared to RAMBO alone. (**e**) Quantification of viral gene copy number in CAL27 tumors after systemic RAMBO treatment. Data were analyzed by the paired student's *t*-test and shown are mean HSV-1 gene copy/mg of tumor DNA ± SE ($P < 0.05$) ($n = 6$/group).

Specifically, one out of seven tumors treated with ATN-224 plus RAMBO completely regressed. A single intratumoral injection of RAMBO demonstrated significant decreased tumor growth (median survival of 20 compared to 16 days for RAMBO versus PBS, $P < 0.05$). While treatment with ATN-224 alone also had significant antitumor effects, the combination of ATN-224 and RAMBO showed improved therapeutic efficacy over either agent alone (median survival of 40 versus 27 days for RAMBO versus ATN-224, $P < 0.01$) (Figure 6c,d).

Combination treatment with ATN-224 and RAMBO inhibits tumor angiogenesis and spontaneous lung metastasis

The apparent enhanced antitumor efficacy and survival benefits resulting from combination treatment with ATN-224 and RAMBO was further investigated by immunohistochemical examination for H&E and CD31 staining of CAL27 tumors (Figure 6e). Mice treated with both ATN-224 and RAMBO had significantly increased tumor necrosis (black arrow in Figure 6e). Furthermore, there was a significant difference in inhibition of angiogenesis between RAMBO alone and ATN-224 plus RAMBO-treated tumor ($P < 0.01$) (Figure 6e,f). Similarly, significantly reduced angiogenesis was also observed in UM-SCC-74A subcutaneous tumor bearing mice (Supplementary Figure S2). Treatment with angiogenesis inhibitors and induction of hypoxia is frequently associated with increased tumor cell entry into circulation and metastasis. Thus, we evaluated whether combination treatment with ATN-224 and RAMBO would have an effect in blocking on metastasis in our UM-SCC-74A tumor model (Figure 6g,h). We frequently observe lung metastases in mice subcutaneously implanted with UM-SCC-74A. Thus, we harvested lungs and sectioned amongst the different *in vivo* groups with UM-SCC-74A flank tumors. Significant reduction in the number of mice showing metastasis was observed in mice treated with ATN-224 plus RAMBO compared to PBS treated mice (1/7 versus 5/7 mice, $P < 0.05$) (Figure 6g,h). Taken together, these results indicate that combination treatment with ATN-224 and RAMBO strongly inhibited lung metastasis of SCC and suggests that this combinatorial therapy has global implications for clinical trials in advanced metastatic stage III/IV HNSCC patients.

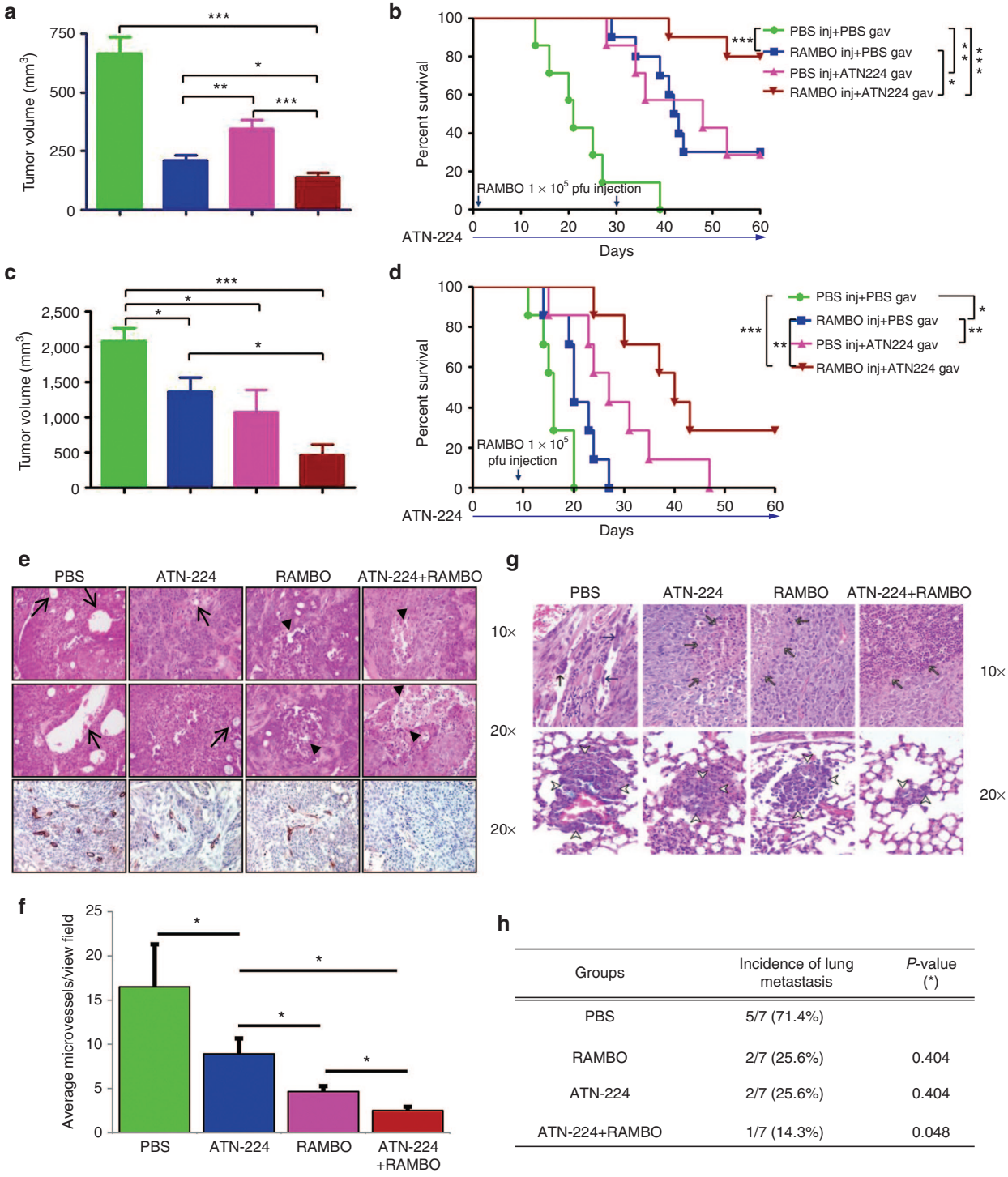

h

Groups	Incidence of lung metastasis	*P*-value (*)
PBS	5/7 (71.4%)	
RAMBO	2/7 (25.6%)	0.404
ATN-224	2/7 (25.6%)	0.404
ATN-224+RAMBO	1/7 (14.3%)	0.048

Figure 6 *In vivo* antitumor effect of the combination treatment with ATN-224 and RAMBO (**a**). Subcutaneously implanted tumors derived from CAL27 (**a,b**) and UM-SCC-74A (**c,d**) cells were treated with PBS, or ATN-224 by daily gavage, when tumor size reached around 150 mm^3. Seven days later from ATN-224 treatment, mice were treated with PBS or RAMBO (1×10^5 pfu on day 1 and day 28 for CAL27 and 1×10^6 pfu on day 7 for UM-SCC-74A) and tumor volume was monitored over time. On day 15 after treatment, the tumor sizes were compared (**a** and **c**). RAMBO combined with ATN-224 significantly enhanced antitumor effect compared to the treatment with ATN-224 or RAMBO alone. (**b** and **d**) Kaplan-Meier survival curves following same treatments. The percentage of surviving mice was determined by monitoring the death of mice (tumor size > 1,000 mm^3) over a period of 60 days. There was a statistically significant longer survival in mice treated with combination therapy ($P < 0.05$). The arrows indicate the time of RAMBO injection and ATN-224 treatment. (**e**) Representative histological characterization of CAL27 xenograft tumor after treatment of 1 week is displayed in Figure 6**a** and **b**. Control (PBS) tumor tissue showed dilated blood vessels and microvessels (arrows). ATN-224 treated tumor exhibited fewer microvessels and some necrotic foci (arrow heads). Tumors from mice treated with both RAMBO and ATN-224 showed more extensive necrosis and reduced blood vessel density than RAMBO alone treated tumors. (**f**) Quantification of CD31 immunostained vessels. There was significant difference in microvessel numbers between PBS control and ATN-224 treatment ($n = 3$/group) ($P < 0.01$). Combination of ATN-224 and RAMBO further reduced microvessel number than RAMBO treated alone (PBS versus ATN-224, $P = 0.015$; PBS versus RAMBO, $P = 0.015$; RAMBO versus ATN-224+RAMBO, $P = 0.033$, PBS versus ATN224+RAMBO, $P = 0.01$). (**g**) The proportion of lung metastases noted in UM-SCC-74A flank tumor model with the different treatment paradigms. (**h**) Table for lung metastasis incidence of subcutaneously implanted UM-SCC-74A tumor ($n = 7$/group). Data were analyzed by the paired student's *t*-test.

DISCUSSION

Oncolytic herpes simplex virus (oHSV) has been widely used in clinical trials and proven to be safe with minimal dose-limiting toxicities. However, the effectiveness of oHSVs in patients has not lived up to the expectations generated from the results observed in preclinical studies.[19] Combing oHSV with chemotherapeutic agents presents an opportunity to increase oncolytic activity by either bolstering virus replication or suppressing systemic innate immune responses that can lead to rapid virus clearance.[20,21] Despite augmenting virus replication, combination of oncolytic viral therapy with chemotherapy has only been well tolerated with few dose limiting toxicities.[6,22,23] While these studies have remain promising, a better elucidation of factors that can limit *in vivo* efficacy of oHSV vectors can help design improved treatment strategies.

Our *in vitro* and *in vivo* assays demonstrated that physiological levels of copper inhibit oHSV therapeutic efficacy. Average serum copper concentrations in adults are ~18–20 µmol/l[24] and our *in vitro* data reveal that concentrations of copper above 8–10 µmol/l inhibits oHSV infection and replication. Based on this finding, we speculated that physiologic copper significantly hinders oHSV therapeutic efficacy in clinical trials. Therefore, we hypothesized that by reducing serum copper levels, we can improve systemic delivery and replication of oHSV, resulting in enhanced therapeutic efficacy.

ATN-224, bis (2-hydroxyethyl) trimethylammonium, is a second-generation analog of ammonium terathiomolybdate (TM) that is US Food and Drug Administration approved for Wilson's disease. The drug is orally available and sustained copper reduction is well tolerated. Copper chelation in humans with ATN-224 is also a safe and effective method of reducing physiologic levels of copper such that it inhibits angiogenesis but not basic cell cycle functioning. Additionally, ATN-224 has been shown to have copper independent antiangiogenic effects[25,26] by directly inhibiting tumor cell invasion and inducing cancer cell anoikis.[27] Its anticancer efficacy has also been imparted to the inhibition of SOD1 and multiple cofactors of the angiogenesis cascade[28] and is currently being investigated as an anticancer agent in several clinical trials (NCT00383851, NCT00405574). Furthermore, the usage of ATN-224 has been approved in Europe.

Here, we tested the impact of an oHSV that encodes for an antiangiogenic gene on head and neck squamous cell carcinoma (HNSCC) alone and in combination with ATN-224. RAMBO is an oHSV that encodes for antiangiogenic Vstat120 and has shown therapeutic efficacy against brain tumors in mice.[12] In this study, we showed that HNSCC is sensitive to RAMBO-induced viral replication and cell killing and RAMBO can be an effective treatment strategy for head and neck cancer. Moreover, the addition of ATN-224 greatly enhanced serum stability, viral replication, and cell killing of RAMBO, resulting in enhanced mice survival and decreased lung metastasis. While we have shown increased serum stability of RAMBO in mice treated with ATN-224, we have not tested its systemic delivery efficacy in HNSCC bearing mice *in vivo*. Future studies evaluating systemic delivery efficacy, safety, and biodistribution for HNSCC will be needed before its clinical investigation in patients.

This study is limited by the lack of testing in an immunocompetent host, which has been documented to play a major role in oncolytic viral clearance. ATN-224 and its parent compound, TM, is a triple threat when used in combination with oHSV therapy. As we demonstrated here, reduction of physiologic levels of copper significantly enhances oHSV therapy through (i) reduction of direct copper mediated inhibition of oHSV, (ii) decreased angiogenesis leading to reduced tumor growth and viral clearance; (iii) increased oHSV replication and cell killing. Decreased angiogenesis and increased viral replication may be able to overcome viral clearance prompted by the innate immune response.

In conclusion, these experiments support the future use of ATN-224 in combination with oHSV for HNSCC. We plan to pursue phase 1 clinical trials as further testing in patients will uncover the potential of combining oHSV with ATN-224, which has the ability to make significant improvements in efficacy of oncolytic viral therapy.

MATERIALS AND METHODS

Reagents

ATN-224, choline tetrathiomolybdate, was kindly provided by Dr. Andrew P. Mazar (Chemistry of Life Processes Institute, Northwestern University, Evanston, IL). ATN-224 stocks (50 mg/ml) were prepared in water, aliquoted, and frozen until use. ATN-224 was diluted to the desired concentration using PBS or medium just before use. For *in vitro* experiments, ascorbate buffer was used as a reducing agent as described.[29] Copper chloride ($CuCl_2 \cdot H_20$) and ascorbic acid were obtained from Sigma (St Louis, MO).

Cell culture and oncolytic viruses

Six human squamous cell carcicnoma (SCC) cell lines (UM-SCC-74A, UM-SCC-1, UM-SCC-11A, UM-SCC-47, UD-SCC-2, and ATCC CAL 27) were used and cultured in Dulbecco modified Eagle medium (DMEM, Gibco/Invitrogen, Carlsbad, CA) supplemented with 10% heat inactivated fetal bovine serum (FBS, Gibco/Invitrogen), 50 µg/ml of penicillin G, 50 µg/ml of streptomycin sulfate, and 1× MEM NEAA (Gibco/ Invitrogen). Vero (African green monkey kidney cells, ATCC) cells were maintained in DMEM containing 10% FBS without 1× MEM NEAA. All cell lines were maintained at 37 °C in a humidified atmosphere at 5% CO_2.

The construction and generation of both control rHSVQ1 and RAMBO (Rapid Antiangiogenesis Mediated By Oncolytic Virus) viruses have been previously described.[30] Viruses were propagated in Vero cells, purified, and infectious virus titers (plaque forming unit per ml (pfu/ml)) were determined by standard plaque forming unit assay on Vero cells.[31,32]

Western blot analysis

Immunoblots were probed with rabbit anti-N-terminal BAI1[33] to probe for Vstat120 or mouse anti-human GAPDH (Abcam, Cambridge, MA), followed by goat anti-rabbit (Dako, Carpinteria, CA) or sheep anti-mouse (Amersham Biosciences, Pittsburgh, PA) as secondary antibodies. The immunoreactive bands were visualized using an enhanced chemiluminescence (GE Healthcare, Piscataway, NJ).

Cytotoxicity assay

Cells were seeded into a 96-well plate (2% FBS media), and were infected with oHSV at the indicated multiplicity of infection (MOI) preincubated with ascorbate buffer ± copper (1 mg/l) ± ATN-224 (32 µmol/l) for 30 minutes at RT. Forty-eight hours postinfection, cell viability was measured using a standard crystal violet assay as described.[30]

In vitro viral replication assays

Cells were seeded into six-well plates, and were infected with oHSV in three groups: RAMBO only (0.1 MOI), RAMBO + Cu (virus 0.1 MOI + copper 20 µmol/l) and RAMBO + Cu + ATN-224 (virus 0.1 MOI + copper 20 µmol/l+ ATN-224 32 µmol/l). Infection proceeded for 2 hours, and then unbound virus was washed away and fresh 2% FBS DMEM media was added to each well. Forty-eight hours post-oHSV infection, cells and media were harvested and the amount of infectious virus particles were determined by performing a standard plaque forming unit assay on Vero cells, as previously described.[29]

Animal xenograft

All mice studies were performed in accordance with the Subcommittee on Research Animal Care at The Ohio State University guidelines, and have been approved by the Institutional Review Board. Four- to 5-week-old female athymic nu/nu mice (NIH-NCI) were injected subcutaneously with 1.5×10^7 of UM-SCC-74A or CAL27 in 100 µl volume into the rear flank. When tumors reached average size of 150 mm^3, mice were randomized to receive either ATN-224 (0.7 mg per day for each mouse) or sterile PBS, delivered by daily

oral gavage. At day 7 from gavage, RAMBO (2×10^6 pfu) or PBS was administered by direct intratumoral injection. The ATN-224 and PBS treatment was continued until the end of the experiment and the tumor volume was calculated using the following formula: Volume = 0.5 LW^2, where W and L are the two maximum dimensions. Measurements of tumor volumes were taken as indicated, and mice were killed when tumor volumes exceeded 2,000 mm^3 or >20% of body mass was lost.

Ceruloplasmin assay

Ceruloplasmin levels were measured weeks 1, 2, 4, and 6 during the study period. Nontumor bearing mice were treated with ATN-224 (0.7 mg/kg) or PBS by daily gavage and blood was collected from facial vein every weeks. Ceruloplasmin was assayed based on its oxidase activity. Two tubes each containing 25 µl mouse serum and 375 µl of 0.1 mol/l sodium acetate buffer (pH 5.0) were incubated for 5 minutes in a 30 °C water bath. Prewarmed 100 µl o-dianisidine dihydrochloride solution (7.88 mmol/l; Sigma) was then added to each tube and the reaction was allowed to continue for 5 minutes in one tube and 15 minutes in the other. Finally, the reaction was quenched by adding 1 ml of 9 mol/l sulphuric acid. The absorbance of both tubes was measured at 540 nm using Beckman Coulter DU 530 spectrophotometer. Ceruloplasmin concentration in IU was calculated using the formula ceruloplasmin oxidase activity = (A15–A5) × 0.625 units/ml, where A5 and A15 are the absorbance at 5 and 15 minutes, respectively.

Ex vivo and *in vivo* serum rescue assay

For *ex vivo* serum rescue assay, CAL27 tumor-bearing mice were treated with ATN-224 (0.7 mg/kg) or PBS by daily gavage. On day 14 after ATN-224 treatment, blood was collected from facial vein and serum was harvested as described.[34] Twenty microliters of serum diluted with 20 µl of Hank's buffered salt solution (HBSS) were incubated with RAMBO (2×10^3 pfu) for 1 hour at 37 °C, and the amount of virus particles was measured by a standard plaque forming unit assay on Vero cells. This assay was run using serial diluted RAMBO and plaque versus pfu number was plotted to give the linear regression standard curve. For *in vivo* serum rescue assay, mice were fed with PBS/ATN-224 (0.7 mg/kg) for 10 days and then RAMBO (5×10^6 pfu) was administered by tail vein injection. Twenty minutes postvirus injection, serum was harvested and the number of infectious virus particles present was determined.

Viral gene copy assay

To measure systemic oHSV (RAMBO) delivery efficacy *in vivo*, quantitative real time PCR analysis of viral gene copy was determined. CAL27 tumor-bearing mice were treated with ATN-224 (0.7 mg/kg) or PBS by daily gavage and injected with RAMBO (5×10^6 pfu) intravenously by a tail vein injection on day 14 after the initial ATN-224 treatment. Two days later from virus injection, tumors were harvested, and total DNA was purified using the Master PureTM Complete DNA & RNA Purification Kit (Cat. No. MC85200, Epicentre Biotechnologies, Madison, WI). A pK1-2 plasmid containing the ICP4 HSV-1 viral gene was kindly provided by Dr. Deborah Parris at The Ohio State University and the following ICP4 primers were used: sense, 5′-CGACACGGATCCACGACCC-3′ and antisense, 5′-GATCCCCCTCCCGCGCTTCGTCCG-3′. Viral gene copy present in the tumors was measured by determining the total number of copies of the HSV-specific ICP4 gene using absolute quantitative real-time PCR (qPCR) analysis. A linear regression curve was generated by diluting the plasmid to various concentrations ranging from 0.001 µg/5 µl to 1 µg/5 µl DNA. The number of plasmids per µg of DNA was calculated by determining the µg of DNA per plasmid using the total number of nucleotides in the plasmid ((amount(ng)* 6.022×10^23)/(length * 1×10^9 * 660)). QPCR with the diluted concentrations of the plasmid was performed as previously described and the CT value versus copy number (Log transformed) was plotted to give a linear regression standard curve. The linear regression line formula generated was used to calculate the oHSV gene copy number.

Evaluation of tumor xenograft by histological analysis

Tumor tissues were fixed in 4% paraformaldehyde, embedded in paraffin and cut into 5-µm sections. Representative sections were stained with Hematoxylin and Eosin (H&E), and then examined by light microscopy. For immunohistochemistry of CD31, sections were stained using antimouse CD31 antibody at a 1:250 dilution (BD PharMingen, San Jose, CA). Appropriate negative and positive controls were done. The total number of stained vessels was determined in five random high-power fields (×400 magnification), and then the mean was reported in a blinded fashion for each tumor.

Lung metastasis

At the time of dissection, lungs were excised and tumor nodules were evaluated. Lung tissues were fixed in 4% paraformaldehyde for 2 days, and 5-micrometer tissue sections were cut and stained with H&E. The entire sections were examined microscopically at low powers (×40 and ×100 magnifications) for the presence of metastases.

Statistical analysis

GraphPad software was used for all statistical analysis. Data are presented as mean ± SD. Data were analyzed using unpaired, two-tailed *t*-tests when comparing two variables. ANOVA with Tukey's post-test was used to compare data in experiments where more than two variables were compared simultaneously.

CONFLICT OF INTEREST

The authors declared no conflict of interest.

ACKNOWLEDGMENTS

The project described was supported by Award Number UL1RR025755 to M.O. from the National Center For Advancing Translational Sciences and R01CA150153 and R01NS064607 to B.K. from NIH and by The Joan Bisesi Memorial Career Development Grant to M.O. The content is solely the responsibility of the authors and does not necessarily represent the official views of the National Center For Advancing Translational Sciences or the National Institutes of Health.

REFERENCES

1. Shiboski, CH, Schmidt, BL and Jordan, RC (2005). Tongue and tonsil carcinoma: increasing trends in the U.S. population ages 20-44 years. *Cancer* **103**:1843–1849.
2. Forastiere, AA, Trotti, A, Pfister, DG and Grandis, JR (2006). Head and neck cancer: recent advances and new standards of care. *J Clin Oncol* **24**: 2603–2605.
3. Harrington, KJ, Hingorani, M, Tanay, MA, Hickey, J, Bhide, SA, Clarke, PM *et al.* (2010). Phase I/II study of oncolytic HSV GM-CSF in combination with radiotherapy and cisplatin in untreated stage III/IV squamous cell cancer of the head and neck. *Clin Cancer Res* **16**: 4005–4015.
4. Le Boeuf, F and Bell, JC (2010). United virus: the oncolytic tag-team against cancer! *Cytokine Growth Factor Rev* **21**: 205–211.
5. Gil, Z, Rein, A, Brader, P, Li, S, Shah, JP, Fong, Y *et al.* (2007). Nerve-sparing therapy with oncolytic herpes virus for cancers with neural invasion. *Clin Cancer Res* **13**: 6479–6485.
6. Mace, AT, Ganly, I, Soutar, DS and Brown, SM (2008). Potential for efficacy of the oncolytic Herpes simplex virus 1716 in patients with oral squamous cell carcinoma. *Head Neck* **30**: 1045–1051.
7. Cox, C, Teknos, TN, Barrios, M, Brewer, GJ, Dick, RD and Merajver, SD (2001). The role of copper suppression as an antiangiogenic strategy in head and neck squamous cell carcinoma. *Laryngoscope* **111**(4 Pt 1): 696–701.
8. Cox, C, Teknos, TN, Barrios, M, Brewer, GJ, Dick, RD and Merajver, SD (2001). The role of copper suppression as an antiangiogenic strategy in head and neck squamous cell carcinoma. *Laryngoscope* **111**(4 Pt 1): 696–701.
9. Büntzel, J, Bruns, F, Glatzel, M, Garayev, A, Mücke, R, Kisters, K *et al.* (2007). Zinc concentrations in serum during head and neck cancer progression. *Anticancer Res* **27**(4A): 1941–1943.
10. Zhang, W, Fulci, G, Buhrman, JS, Stemmer-Rachamimov, AO, Chen, JW, Wojtkiewicz, GR *et al.* (2012). Bevacizumab with angiostatin-armed oHSV increases antiangiogenesis and decreases bevacizumab-induced invasion in U87 glioma. *Mol Ther* **20**: 37–45.
11. Goodwin, JM, Schmitt, AD, McGinn, CM, Fuchs, BC, Kuruppu, D, Tanabe, KK *et al.* (2012). Angiogenesis inhibition using an oncolytic herpes simplex virus expressing endostatin in a murine lung cancer model. *Cancer Invest* **30**: 243–250.
12. Yoo, JY, Pradarelli, J, Haseley, A, Wojton, J, Kaka, A, Bratasz, A *et al.* (2012). Copper chelation enhances antitumor efficacy and systemic delivery of oncolytic HSV. *Clin Cancer Res* **18**: 4931–4941.
13. Clewell, A, Barnes, M, Endres, JR, Ahmed, M and Ghambeer, DK (2012). Efficacy and tolerability assessment of a topical formulation containing copper sulfate and hypericum perforatum on patients with herpes skin lesions: a comparative, randomized controlled trial. *J Drugs Dermatol* **11**: 209–215.

14. Shishkov, S, Varadinova, T, Panteva, M and Bontchev, P (1997). Effect of complexes of zinc, cobalt and copper with D-aminosugars on the replication of herpes simplex virus type 1 (HSV-1). *Met Based Drugs* **4**: 35–38.
15. Panteva, M, Varadinova, T and Turel, I (1998). Effect of copper acyclovir complexes on herpes simplex virus type 1 and type 2 (HSV-1, HSV-2) infection in cultured cells. *Met Based Drugs* **5**: 19–23.
16. Doñate, F, Juarez, JC, Burnett, ME, Manuia, MM, Guan, X, Shaw, DE *et al.* (2008). Identification of biomarkers for the antiangiogenic and antitumour activity of the superoxide dismutase 1 (SOD1) inhibitor tetrathiomolybdate (ATN-224). *Br J Cancer* **98**: 776–783.
17. Mao, S and Huang, S (2013). Zinc and copper levels in bladder cancer: a systematic review and meta-analysis. *Biol Trace Elem Res* **153**: 5–10.
18. Crowe, A, Jackaman, C, Beddoes, KM, Ricciardo, B and Nelson, DJ (2013). Rapid copper acquisition by developing murine mesothelioma: decreasing bioavailable copper slows tumor growth, normalizes vessels and promotes T cell infiltration. *PLoS ONE* **8**: e73684.
19. Friedman, GK, Raborn, J, Kelly, VM, Cassady, KA, Markert, JM and Gillespie, GY (2013). Pediatric glioma stem cells: biologic strategies for oncolytic HSV virotherapy. *Front Oncol* **3**: 28.
20. Aghi, M, Rabkin, S and Martuza, RL (2006). Effect of chemotherapy-induced DNA repair on oncolytic herpes simplex viral replication. *J Natl Cancer Inst* **98**: 38–50.
21. Peng, KW, Myers, R, Greenslade, A, Mader, E, Greiner, S, Federspiel, MJ *et al.* (2013). Using clinically approved cyclophosphamide regimens to control the humoral immune response to oncolytic viruses. *Gene Ther* **20**: 255–261.
22. Cinatl, J Jr, Cinatl, J, Michaelis, M, Kabickova, H, Kotchetkov, R, Vogel, JU *et al.* (2003). Potent oncolytic activity of multimutated herpes simplex virus G207 in combination with vincristine against human rhabdomyosarcoma. *Cancer Res* **63**: 1508–1514.
23. Freytag, SO, Stricker, H, Pegg, J, Paielli, D, Pradhan, DG, Peabody, J *et al.* (2003). Phase I study of replication-competent adenovirus-mediated double-suicide gene therapy in combination with conventional-dose three-dimensional conformal radiation therapy for the treatment of newly diagnosed, intermediate- to high-risk prostate cancer. *Cancer Res* **63**: 7497–7506.
24. Ford, ES (2000). Serum copper concentration and coronary heart disease among US adults. *Am J Epidemiol* **151**: 1182–1188.
25. Lowndes, SA, Adams, A, Timms, A, Fisher, N, Smythe, J, Watt, SM *et al.* (2008). Phase I study of copper-binding agent ATN-224 in patients with advanced solid tumors. *Clin Cancer Res* **14**: 7526–7534.
26. Juarez, JC, Betancourt, O Jr, Pirie-Shepherd, SR, Guan, X, Price, ML, Shaw, DE *et al.* (2006). Copper binding by tetrathiomolybdate attenuates angiogenesis and tumor cell proliferation through the inhibition of superoxide dismutase 1. *Clin Cancer Res* **12**: 4974–4982.
27. Kumar, P, Yadav, A, Patel, SN, Islam, M, Pan, Q, Merajver, SD *et al.* (2010). Tetrathiomolybdate inhibits head and neck cancer metastasis by decreasing tumor cell motility, invasiveness and by promoting tumor cell anoikis. *Mol Cancer* **9**: 206.
28. Lin, J, Zahurak, M, Beer, TM, Ryan, CJ, Wilding, G, Mathew, P *et al.* (2013). A non-comparative randomized phase II study of 2 doses of ATN-224, a copper/zinc superoxide dismutase inhibitor, in patients with biochemically recurrent hormone-naïve prostate cancer. *Urol Oncol* **31**: 581–588.
29. Sagripanti, JL, Routson, LB, Bonifacino, AC and Lytle, CD (1997). Mechanism of copper-mediated inactivation of herpes simplex virus. *Antimicrob Agents Chemother* **41**: 812–817.
30. Hardcastle, J, Kurozumi, K, Dmitrieva, N, Sayers, MP, Ahmad, S, Waterman, P *et al.* (2010). Enhanced antitumor efficacy of vasculostatin (Vstat120) expressing oncolytic HSV-1. *Mol Ther* **18**: 285–294.
31. Terada, K, Wakimoto, H, Tyminski, E, Chiocca, EA and Saeki, Y (2006). Development of a rapid method to generate multiple oncolytic HSV vectors and their *in vivo* evaluation using syngeneic mouse tumor models. *Gene Ther* **13**: 705–714.
32. Sundaresan, P, Hunter, WD, Martuza, RL and Rabkin, SD (2000). Attenuated, replication-competent herpes simplex virus type 1 mutant G207: safety evaluation in mice. *J Virol* **74**: 3832–3841.
33. Kaur, B, Brat, DJ, Calkins, CC and Van Meir, EG (2003). Brain angiogenesis inhibitor 1 is differentially expressed in normal brain and glioblastoma independently of p53 expression. *Am J Pathol* **162**: 19–27.
34. Wakimoto, H, Ikeda, K, Abe, T, Ichikawa, T, Hochberg, FH, Ezekowitz, RA *et al.* (2002). The complement response against an oncolytic virus is species-specific in its activation pathways. *Mol Ther* **5**: 275–282.

Supplementary Information accompanies this paper on the *Molecular Therapy—Oncolytics* website (http://www.nature.com/mto)